Journal of Thermal Analysis, Vol. 1 (1969) 75–96

Special Reviews

THE APPLICATION OF DIFFERENTIAL THERMAL ANALYSIS TECHNIQUE TO THE STUDY OF SINGLE, BINARY AND TERNARY OXIDE CATALYST SYSTEMS

S. K. BHATTACHARYYA and N. C. DATTA

Department of Chemistry, Indian Institute of Technology, Kharagpur, India

(Received February 4, 1969)

The authors have reviewed the salient features of the thermal behavior of the following systems:

(A) Single oxide systems: (i) Cr_2O_3, (ii) Fe_2O_3, (iii) Al_2O_3, (iv) MnO_2, (v) ZrO_2, (vi) NiO, (vii) ZnO, (viii) TiO_2, (ix) SiO_2, (x) ThO_2.

(B) Binary oxide systems: (i) $Cr_2O_3-Al_2O_3$, (ii) $Cr_2O_3-Fe_2O_3$, (iii) Cr_2O_3-ZnO, (iv) $Al_2O_3-SiO_2$, (v) $Al_2O_3-Fe_2O_3$, (vi) $MnO-Cr_2O_3$, (vii) $Cu-Al_2O_3$, (viii) $ZrO_2-Cr_2O_3$, (ix) $NiO-Cr_2O_3$, (x) ZrO_2-NiO, (xi) $ThO_2-Al_2O_3$.

(C) Ternary oxide systems: (i) $NiO-Cr_2O_3-ZrO_2$, (ii) $Fe_2O_3-Cr_2O_3-Al_2O_3$.

(D) Vanadates: (i) tin vanadate, (ii) copper vanadate, (iii) lead vanadate, (iv) cobalt vanadate and (v) silver vanadate.

Excellent correlations have been obtained in most of the systems between the thermal characteristics of the solids, as revealed by DTA, and their specific surface areas and catalytic activity.

I. Introduction

The technique of differential thermal analysis (DTA) has been used for a long time to the study of thermal processes in solids like clays, minerals, various inorganic and organic compounds, etc. This method of thermal analysis has been regarded as a valuable adjunct to the other more sophisticated physical methods as X-ray analysis, adsorption measurements, spectroscopic studies, magnetic susceptibility determinations, etc. for the study of the structural characteristics of a solid. In course of a thermal treatment while the above-mentioned physical methods clearly depict the characteristics of the solid only in the initial, final and in some other convenient intermediate states, by the DTA technique a continuous record of the various changes within the solid can be made with rise in temperature.

It is now conclusively established that the structural properties of the solid phase play an important role in heterogeneous catalysis. In order to elucidate the phenomenon of heterogeneous catalysis into a more clear understanding, Bhattacharyya et al. [1–13] have introduced the technique of DTA in conjunction with other physical methods like X-ray analysis and surface area determinations by the BET (Brunauer–Emmett–Teller) method to the study of the thermal behaviour of a large number of catalyst systems of both theoretical and technical importance.

By such studies a useful correlation between the DTA results, surface area measurements and catalytic activity has been obtained in almost all systems.

In this paper, the authors have reviewed the results of such systematic and exhaustive observations, and also the correlations of the thermal behaviour of these systems with their surface area and catalytic activity.

II. Experimental

The experimental arrangement of the DTA-apparatus and the procedure have been described earlier in detail by Bhattacharyya and Ramchandran [4].

The surface areas of all the systems were measured by the well-known BET technique.

The single and the mixed oxide systems were prepared by a number of methods under varying conditions. The general method was to add NH_4OH, NaOH or KOH to an aqueous solution of the salt at different concentrations, temperature, pH, etc. The precipitate was washed with water until free from the adhering ions and then oven-dried at 110° for several hours. The effect of ageing and drying temperature was also studied. In this paper, the results from the freshly-prepared gels obtained by adding NH_4OH to the aqueous solution of the metal nitrate and then oven-dried at 110° after a thorough washing will be presented in general.

The vanadates were prepared using a number of methods. A small variation in the experimental conditions yielded frequently an entirely different precipitate. The details of the methods of preparation along with the methods of chemical analysis of the precipitates have been reported recently [12, 13].

III. Results and discussion

1. *Single oxide systems*

Excellent correlations have been obtained in all the single oxide systems between the thermal characteristics of the oxides, their surface area and catalytic activity. Maximum catalytic activity and maximum surface area have been found to correspond to the temperature where the gel gets dehydrated and phase transition starts. Bhattacharyya et al [1–3] have studied numerous single oxide systems, namely, Cr_2O_3, Fe_2O_3, Al_2O_3, ZrO_2, ThO_2, NiO, ZnO, TiO_2, MnO_2, SiO_2. All these systems have been reviewed in detail earlier [9] and in this section a brief discussion of these systems will be presented.

The results of DTA and surface area measurements of some of these systems are given in Table 1 and the thermograms of all these systems are represented in Fig. 1.

(i) Chromic oxide: As evident from Fig. 1, there are two endothermic peaks in the thermogram at 160° and 250° which are due to the removal of loosely bound and rigidly bound water, respectively. The exothermic peak at 395° originates

from the crystallization of Cr_2O_3. Surface area measurements indicate that the system has a maximum surface area (187.5 m^2/g, Table 1) at 300°. The exothermic peak is absent in the DTA thermogram of the system in nitrogen atmosphere. Obviously, the crystallization of Cr_2O_3 proceeds via some oxidation reaction. As suggested by Griffith et al [14, 15] from the electrical conductivity measurements

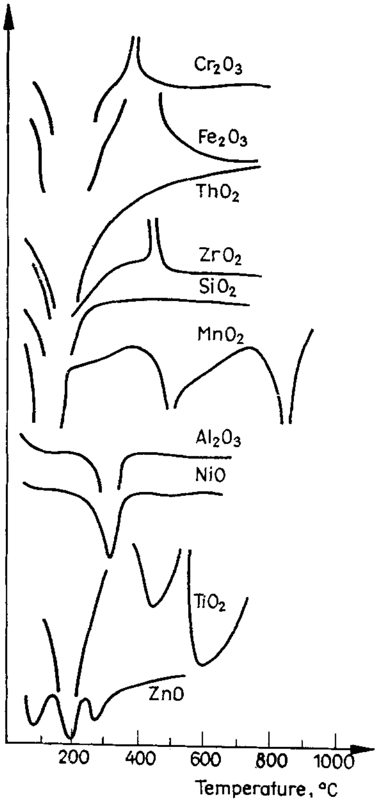

Fig. 1. DTA curves of single oxide gels

of Cr_2O_3 and by Domine-Burges [16] from the thermogravimetric studies, it may be the fact that in air, excess O^{2-} ions are added at the surface of Cr_2O_3 and, due to the presence of excess anions, the average valency of the surface chromium ions is raised to a higher valence, and the p-type behaviour of Cr_2O_3 becomes more predominant. The transition to more p-typeness from more n-typeness and large surface area of the catalyst (Table 1) can explain the maximum activity of Cr_2O_3 for hydrogenation reaction in the temperature range 350–370°. It has been recently reported from E.S.R. studies by a number of workers that the activity of Cr_2O_3 catalyst is due to the presence of Cr^{5+} ions.

Table 1

System	Endothermic peak temp. °C	Exothermic peak temp.^{b} °C	Surface area^c (m^2/g)				
Cr_2O_3	160	395	235.9	301.0	315.3	263.2	223.1
	250		(100)	(200)	(300)	(350)	(400)
Fe_2O_3	180	420	46.8	47.5	49.2	24.4	22.8
			(110)	(200)	(250)	(300)	(400)
Al_2O_3	120	—	2	205	235	200	170
	330		(290)	(350)	(380)	(430)	(480)
ZrO_2	170	430		175.0	177.5	182.9	147.4
				(200)	(300)	(350)	(400)

a Due to dehydration
b Due to crystallization
c Figure within bracket represents the temperature in °C at which the surface area was measured.

(ii) Ferric oxide: It is seen from the DTA thermogram of Fe_2O_3 gel shown in Fig. 1 that the gel gets dehydrated in the temperature range 100–270° and the exothermic transition from amorphous to crystalline α-Fe_2O_3 occurs at 420°. X-ray analysis supports this observation. The surface area of the gel passes through a maximum value of 49.2 m^2/g (Table 1) at 250° when the dehydration is complete and it is anticipated that Fe_2O_3 should show maximum catalytic activity at this temperature region. X-ray analysis of the samples aged for about 90 days showed the presence of both α-Fe_2O_3 and α-$Fe_2O_3 \cdot H_2O$ (goethite) and the exothermic peak for crystallization was absent in the DTA thermograms of such aged samples.

(iii) Alumina: The endothermic peaks at 120° and 330° (Fig. 1) are due to the dehydration of the gel leading to the formation of γ-Al_2O_3. The dehydration product at 330° indicated X-ray patterns of both γ-modification and ill-defined Θ-modification. γ-Al_2O_3 passes to α-Al_2O_3 above 900° via the Θ-modification and the small endothermic peak between 450–500° may be due to the transformation of γ-Al_2O_3 to Θ-Al_2O_3 which has been recently reported in literature by X-ray diffraction studies.

The surface area of alumina gels passes through the maximum value (235 m^2/g), as seen from Table 1, at 380° and this may be the reason for the efficient activity of γ-Al_2O_3 as a dehydration catalyst at this temperature range.

(iv) Manganese dioxide: MnO_2, prepared by adding $KMnO_4$ to a solution of manganous sulphate, indicates three endothermic peaks in its DTA thermogram (Fig. 1). The peak at 130° is due to the loss of water whereas the formations of bixbyite (Mn_2O_3) and hausmannite (Mn_3O_4) give rise to the endothermic peaks

at 550° and 940° respectively. But these oxides, Mn_2O_3 and Mn_3O_4, are not the cause of the catalytic properties of MnO_2, as pointed out by Berezovskaya and Semikhatova [17]. Some other phase like the poorly-crystalline δ-MnO_2 may be responsible for the catalytic activity of MnO_2 [18]. The absence of the thermal effect at 200–250° due to the formation of δ-MnO_2 may be due to the masking effect originating from the large amount of water present in the MnO_2 gels.

(v) Thoria: ThO_2 heated at 300° has been used as catalyst in various reactions like the synthesis of isobutane from water gas, or the reaction of nitric oxide with hydrogen, or the dehydration of alcohols to olefins. From the DTA thermogram of this oxide shown in Fig. 1, it is evident that the dehydration is complete in the temperature range 70–280° (endothermic peak at 140°) and at about 300° there is an exothermic trend due to crystallization of ThO_2. The DTA-curve of ThO_2 containing 5% K_2CO_3 which is not shown in Fig. 1 exhibited complete absence of the exothermic trend and this retardation of crystallization of ThO_2 by K_2CO_3 explains the promoter action of K_2CO_3 in the catalytic activity of ThO_2 as reported by Pichler and Ziesecke [19].

(vi) Zirconia: The DTA curve of ZrO_2 in Fig. 1 showed one endothermic peak at 170° due to dehydration and one exothermic peak at 430° due to transition of ZrO_2 from amorphous to monoclinic variety. The surface area of the gel passed through a maximum of 182.9 m^2/g at 350° (Table 1) with increasing temperature and the catalytic activity of this gel is also found to decrease above 350°.

(vii) Titania: The DTA-thermogram of this gel in Fig. 1 indicated endothermic loss of water at 190–230° and two exothermic transitions at 375° and 510° probably due to the formation of anatase and brookite forms, respectively. An exothermic trend is shown at about 650° probably due to the transition to the rutile form.

(viii) Silica: There is no other transformation up to 700° except an endothermic dehydration peak at 140°. The DTA-curve is given in Fig. 1.

(ix) Nickel oxide: The two endothermic peaks at 105° and 350° as shown in the DTA thermogram of NiO-gel in Fig. 1 are due to the removal of loosely bound water and to the elimination of one mole of water from $NiO \cdot H_2O$, respectively.

(x) Zinc oxide: The DTA-thermogram of ZnO shown in Fig. 1 exhibits three endothermic peaks. The peak at 80° is due to the elimination of loosely bound water. The peak at 190° is due to the decomposition of $Zn(OH)_2$ to ZnO and the peak at 280° may be due to the formation of a definite hydrate of ZnO.

2. *Binary oxide systems*

Binary oxide systems are generally important catalysts of technical importance because the doping or incorporation of one oxide in another may change the defect nature of the entire solid and hence its semiconductivity. By DTA of these binary systems a mutual stabilizing action against crystallization of any of the components [20–23] is observed nearly in all systems. Either the exothermic peak is vanished or retarded to a higher temperature. That is, the catalyst can retain its amorphous character over a long range of temperature. It has been found also that the catalysts in which there is maximum stabilizing action have maximum surface area and high catalytic activity.

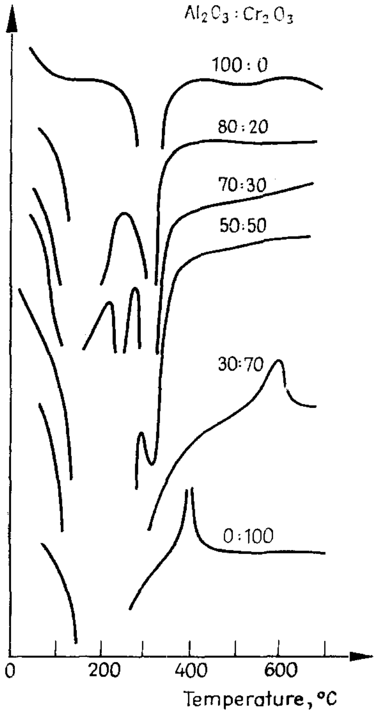

Fig. 2. DTA curves of Cr_2O_3—Al_2O_3 binary gels

(i) Chromic oxide—Alumina: The DTA thermograms of this system (Cr_2O_3—Al_2O_3) are presented in Fig. 2 and the results of DTA, catalytic activity and surface area measurements are summarized in Table 2. As seen from Fig. 2 and Table 2, the presence of Al_2O_3 prevents the crystallization of Cr_2O_3. The exothermic crystallization peak appears at 395° in case of 100% Cr_2O_3, whereas in the system (30 mole% Al_2O_3, 70 mole% Cr_2O_3) it appears at 590°.

The gel containing 30 mole% Cr_2O_3 and 70 mole% Al_2O_3 is most remarkable due to appearance of a small endothermic peak at 244° which may be attributed to the formation of poorly-crystalline δ-Cr_2O_3. It may be pointed out that the magnetic susceptibility per g of the sample is 49.6×10^{-6} for 35% Cr_2O_3 and 22.8 ×

Table 2

Composition (mole percent)		Endothermic peak temp.[a] °C	Exothermic peak temp.[b] °C	Surface area[c] (approx.) (m^2/g)	Conversion of n-heptane to toluene percent	Butadiene yield, percent
Al_2O_3	Cr_2O_3					
100	0	330	—	306	2.8	15.94
80	20	310	—	269	12.5	22.80
69.1	30.9	244[d] 310	—	325	13.1	20.81
49.8	50.2	320	—	275	12.6	19.21
27.1	72.9	—	590	—	14.0	17.96
0	100	—	395	45	7.5	7.97

[a] Due to formation of γ-Al_2O_3

[b] Due to crystallization of Cr_2O_3

[c] Data taken from Griffith et al. [14, 15]

[d] Due to formation of δ-Cr_2O_3

$\times 10^{-6}$ for 100% Cr_2O_3 [24]. Moreover, Griffith et al. [14, 15] have reported that the gel containing 29.6% Cr_2O_3 has the maximum surface area of 325 m^2/g and also, the percentage of conversion of n-heptane to toluene over co-precipitated Cr_2O_3–Al_2O_3 is the highest in the two regions: 30 mole% Al_2O_3, 70 mole% Cr_2O_3 and 70 mole% Al_2O_3, 30 mole% Cr_2O_3. Bhattacharyya and Ganguly [9] when tried the single-step conversion of ethanol to butadiene, observed highest catalytic activity in the gel containing 30 mole% Cr_2O_3 and 70 mole% Al_2O_3. These results can be seen in Table 2. The formation of δ-Cr_2O_3 phase in this gel at 244°, as revealed by DTA, may be responsible for the enhanced catalytic activity, magnetic susceptibility and for an increase in surface area of the system. The results of DTA, surface area measurements and catalytic activity are shown diagrammatically in Fig. 3.

Table 3

Composition (mole percent)		Exothermic peak temp. °C	Surface area (m^2/g)
Cr_2O_3	Fe_2O_3		
0	100	420	49.2
20	80	500	217.5
40	60	550	291.8
60	40	480	168.2
80	20	440	287.1
100	0	395	263.2

(ii) Chromic oxide—Ferric oxide: As discussed earlier (Section III.1), 100% Cr_2O_3 and 100% Fe_2O_3 crystallize at 395° and 420° respectively. From Table 3 and Fig. 4 it is evident that a mutual protective action against crystallization develops when small quantities of one component are added to another. Maximum mutual protective action against crystallization (exothermic peak at 550°) and maximum surface area (291.8 m^2/g) are exhibited by the gel containing 40 mole% Cr_2O_3 and 60 mole% Fe_2O_3.

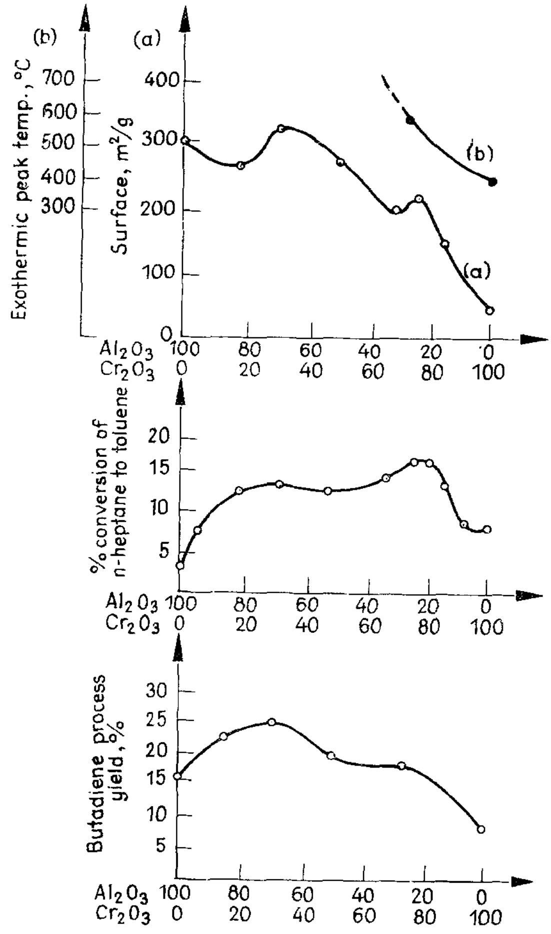

Fig. 3. Correlation between catalytic activity, DTA-results and surface area of Cr_2O_3—Al_2O_3 binary gels

(iii) Chromic oxide–Zinc oxide: The thermograms of a mechanical mixture of Cr_2O_3 and ZnO in 1 : 1 ratio and of this system obtained by co-precipitation

are shown by curves 1 and 2 of Fig. 5a. The low temperature endothermic peaks in curve 2, Fig. 5a are due to dehydration of the system. The exothermic peak at 620°, in case of the mechanical mixture, is due to the formation of spinel, $ZnCr_2O_4$. But there are three exothermic dents at 565°, 665° and 885° after a pronounced exothermic peak at 415° (Fig. 5a, curve 2). These may be due to the stepwise spinel formation. Usually the maximum catalytic activity for such a system is expected at the stage where the bulk is unchanged and tiny crystallites of the spinels have appeared at some points. But the maximum catalytic activity of the Cr_2O_3-ZnO system for the synthesis of methanol under high pressure has been observed at a temperature which is about 200° less than the temperature of

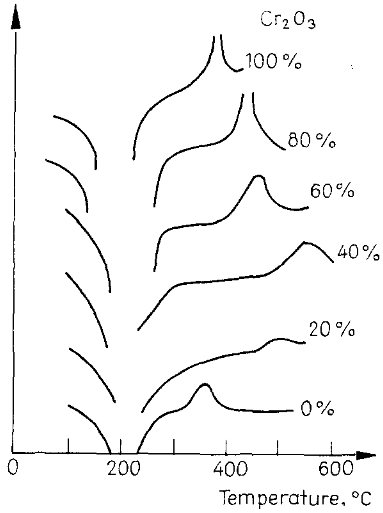

Fig. 4. DTA curves of $Cr_2O_3-Fe_2O_3$ binary gels

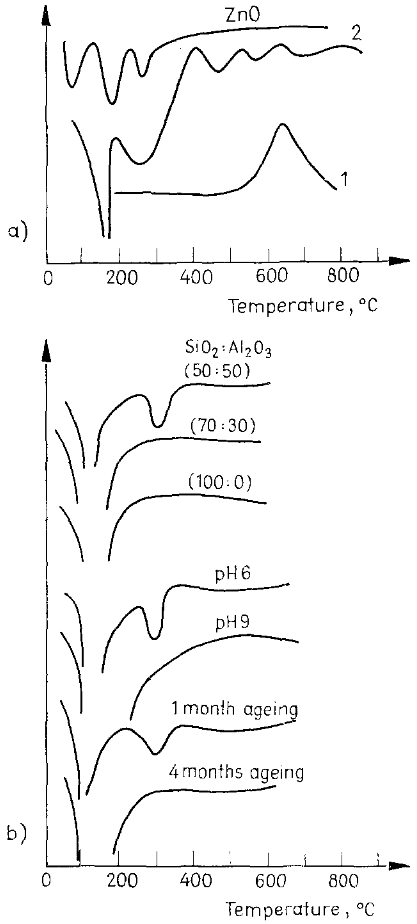

Fig. 5. DTA curves of (a) Cr_2O_3-ZnO and (b) $Al_2O_3-SiO_2$ binary gels

spinel formation. At such low temperatures (about 300°) the spinel phase may not be very deep due to a slow rate of diffusion of ZnO through the surface of the spinel and at high temperatures the rate of spinel formation is stepped up in stages, as seen from the DTA thermogram of the co-precipitated gel, leading to gradual deactivation of the catalyst.

(iv) Alumina – Silica: The synthetic $SiO_2-Al_2O_3$ catalyst predominates the field of the cracking of hydrocarbons. The thermograms of this system are given in Fig. 5b. It is seen that the endothermic peak at 330° due to the formation of γ-Al_2O_3 is absent for the systems containing 30 mole%or less of Al_2O_3. This endothermic peak disappears also when the pH of the medium from which the gel is precipitated is 9 or more, or when the gel is aged for at least 4 months. According to Oblad [25], any positive ion like Na^+ or NH_4^+ present in course of the preparation of such gel interacts with the surface OH groups to give Si–O–Al bonds. The tetracoordination of aluminium thus enforced is highly stabilized by the positive ion, ultimately reading to the aluminate structure. No γ-Al_2O_3 will be formed in such a system except if the alumina-content is high thus decreasing the effective stabilizing area, or if the pH is low causing a decrease in the stabilizing action of the electropositive ion. All these theoretical conclusions have been confirmed by the DTA results as stated above.

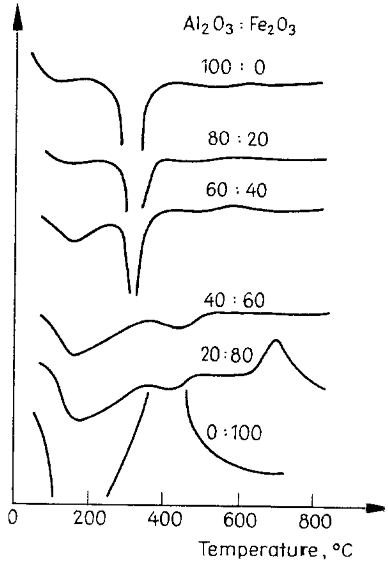

Fig. 6. DTA curves of $Fe_2O_3-Al_2O_3$ binary gels

(v) Alumina – Ferric oxide: The DTA thermograms of this system ($Al_2O_3-Fe_2O_3$) are represented in Fig. 6 and the results of DTA, surface area measurements and

catalytic activity are shown in Table 4 and Fig. 7. $Al_2O_3-Fe_2O_3$ is reported to be a very good catalyst for the oxidation of carbon monoxide to carbon dioxide and for the dehydrogenation of cyclohexane. This catalyst was also tried for the conversion of ethanol to butadiene [9]. As seen from Fig. 6 and Table 4 addition of Al_2O_3 causes a protective action against the formation of crystalline α-Fe_2O_3. The transformation into α-Fe_2O_3 is altogether stopped when 60 mole% or more Al_2O_3 is present in the co-precipitated gel. This system (40% Cr_2O_3–60% Al_2O_3) exhibits also maximum catalytic activity for the conversion of ethanol to butadiene (37.7% at 425°) and maximum surface area, 290 m²/g (Table 4).

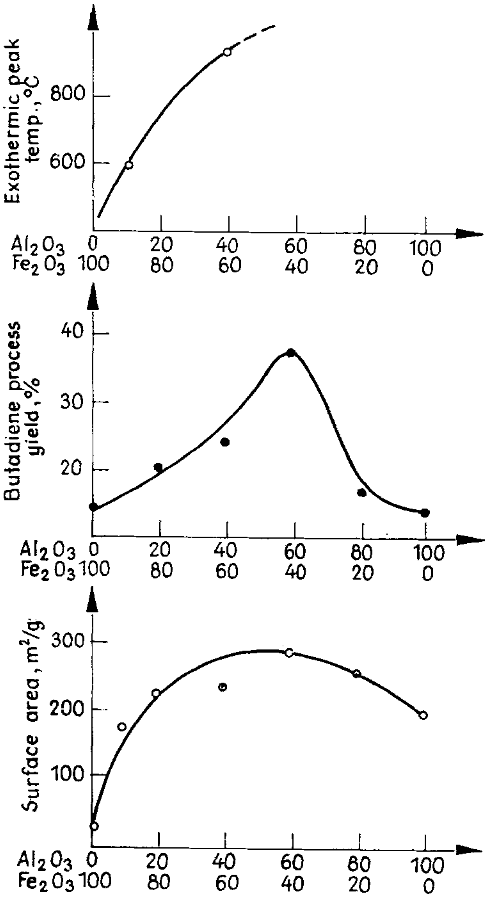

Fig. 7. Correlation between catalytic activity, DTA-results and the surface area of $Fe_2O_3-Al_2O_3$ binary gels

Table 4

Composition (mole percent)		Endothermic peak temp.[a] °C	Exothermic peak temp.[b] °C	Surface area (m^2/g)	Process conversion of ethanol to butadiene percent
Fe_2O_3	Al_2O_3				
100	0	—	420	23.0	14.33
90	10	no peak	605	176.2	—
80	20	420	695	229.5	20.08
60	40	420	930	235.9	23.83
40	60	320	no peak	290.0	37.70
20	80	320	no peak	262.0	16.24
0	100	330	—	200.0	14.94

a Due to formation of γ-Al_2O_3
b Due to formation of α-Fe_2O_3

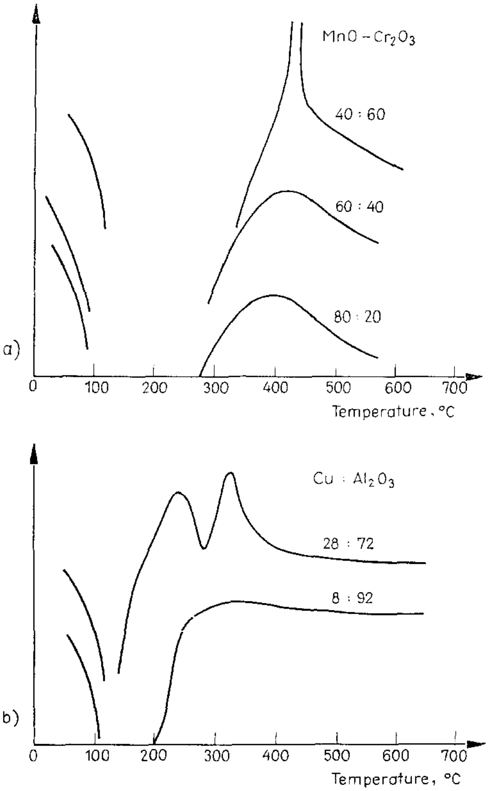

Fig. 8. DTA curves of (a) MnO—Cr_2O_3 and (b) Cu—Al_2O_3 gels

(vi) Manganous oxide – Chromic oxide: Thermograms of the air-dried gels of MnO – Cr_2O_3 co-precipitated from their nitrate solutions with KOH are shown in Fig. 8a. All the samples show an endothermic peak of large magnitude in the temperature range 100 – 350° due to loss of loosely bound and rigidly bound water from the hydrous precipitate. But the crystallization of Cr_2O_3 is considerably affected by the presence of MnO; when MnO-content is 62% or higher, the thermograms (Fig. 8a) do not show the exothermic peak for the crystallization of Cr_2O_3.

(vii) Copper – Alumina: In Fig. 8b are represented the thermal behaviour of Cu - Al_2O_3 gels obtained by adding $(NH_4)_2CO_3$ to $Cu(NO_3)_2$ solution containing Al_2O_3 held in suspension by vigorous agitation and then reduced in H_2 at 250°. All the samples show an endothermic peak at 130° due to removal of water and two exothermic peaks at 200° and 320°, respectively. These exothermic peaks are absent when the DTA is carried out in nitrogen atmosphere indicating that some oxidation reactions occur at these temperatures. Most probably, Cu becomes oxidized to Cu_2O at 200° and then to CuO at 320°. In systems containing 8 mole % Cu these oxidation reactions are inhibited and the exothermic peaks are absent. Ipatieff and Monroe [26] have observed at 290–330° highest catalytic activity in Cu–Al_2O_3 catalysts in the composition-range: 28 – 62% Cu + 72 – 38% Al_2O_3 for the synthesis of methanol from CO and H_2 under pressure. The lowest conversion is obtained with the catalyst containing 8% Cu. It may be pointed out that the highest catalytic activity is obtained at a temperature at which Cu_2O is oxidized to CuO, as revealed by DTA.

(viii) Chromic oxide – Zirconia: Important results of DTA and surface area measurements are given in Table 5 and the DTA thermograms of this system are shown in Fig. 9a. Maximum mutual protective action against crystallization (exo-peak temperature 817°) and maximum surface area (222 m^2/g) are exhibited by the gel containing 40 mole% Cr_2O_3 and 60 mole% ZrO_2.

Table 5

Composition (mole percent)		Exothermic peak temp. °C	Surface area (m^2/g)
Cr_2O_3	ZrO_2		
0	100	430	182.9
20	80	548	186.4
40	60	817	222.0
60	40	770	132.0
80	20	500	197.6
100	0	395	187.5

(ix) Chromic oxide–Nickel oxide: As seen from Fig. 9b representing the DTA thermograms of this system and from Table 6, addition of 20 mole% NiO retards the crystallization of Cr_2O_3 by about 105° and the exothermic peak for crystallization is absent in the gels containing 40 mole% or more of NiO.

(x) Thoria–Alumina: The binary $ThO_2-Al_2O_3$ catalyst is superior to the component single oxides for the synthesis of isoparaffin from carbon monoxide

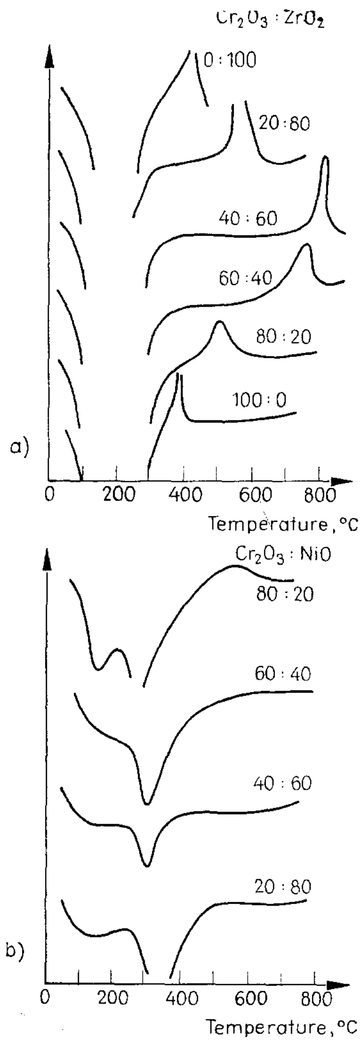

Fig. 9. DTA curves of (a) $ZrO_2-Cr_2O_3$ and (b) $NiO-Cr_2O_3$ binary gels

Table 6

Composition (mole percent)		Exothermic peak temp. °C
Cr_2O_3	NiO	
80	20	500
60	40	Exo-trend only
40	60	absent
20	80	absent

and hydrogen, and small quantities of K_2CO_3 have a good promoter action on such a system [19]. The DTA curves of both mechanical mixture and co-precipitated $ThO_2-Al_2O_3$ (80 : 20) are given in Fig. 10a. It is seen that though the exothermic trend in the thermogram due to crystallization of ThO_2 appears at 500° in case of either co-precipitated system or mechanical mixture of ThO_2 and Al_2O_3 (350° for pure ThO_2), it is not completely absent. But addition of even 0.2% K_2CO_3 totally inhibits the crystallization as shown in Fig. 10a. This probably explains the promoter action of K_2CO_3, and Al_2O_3 probably acts as carrier for the catalyst ThO_2.

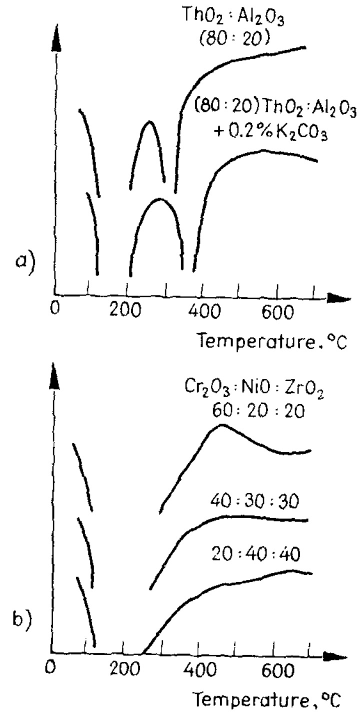

Fig. 10. DTA curves of (a) $ThO_2-Al_2O_3$ binary gels and (b) $NiO-Cr_2O_3-ZrO_2$ ternary gels

(xi) Zirconia–Nickel oxide: It is found from DTA of this system that as the NiO-content increases in the system, the exothermic peak temperature for the crystallization of ZrO_2 also increases. Ultimately the exothermic peak vanishes when 60 mole% of NiO is present. This also illustrates the protective action of NiO on the crystallization of ZrO_2.

3. *Ternary oxide systems*

The following systems have been studied by Bhattacharyya and his coworkers (loc. cit.) and discussed in detail earlier [9]:

(i) $NiO-Cr_2O_3-ZrO_2$
(ii) $Al_2O_3-Fe_2O_3-Cr_2O_3$

Mutual protective action against crystallization is evident in both systems. The system containing 30 mole% NiO, 40 mole% Cr_2O_3 and 30 mole% ZrO_2 is amorphous even up to 600° (Fig. 10b, Table 7). The system $Al_2O_3-Fe_2O_3-Cr_2O_3$ was tried for the conversion of ethanol to butadiene. Important results of DTA, surface area measurements and catalytic activity of this system are summarized in Table 8 and the thermograms are represented in Fig. 11. It can be seen from Table 8 and Fig. 11 that the exothermic peaks of crystallization of Fe_2O_3 and Cr_2O_3 are absent or retarded in a wide range of composition and the highest conversion of ethanol to butadiene takes place on the catalysts: $Al_2O_3 : Fe_2O_3 : Cr_2O_3 = 60 : 10 : 30$ and $40 : 30 : 30$.

Table 7

Composition (mole percent)			Exothermic peak temp. °C
Cr_2O_3	NiO	ZrO_2	
80	10	10	400
60	20	20	470
40	30	30	absent
20	40	40	absent

4. *Vanadates*

The thermograms of some of these vanadates along with the methods of their preparation have been reported recently (loc. cit.). A short discussion of the thermal behaviour of all these vanadates will be presented in this section.

(i) Tin vanadate: The compound is found to have the composition: Sn 29.5%, V 24.94%, NH_3 2% and H_2O 9%, corresponding to a formula $SnV_2O_7 \cdot 2\frac{1}{2} H_2O \cdot \frac{1}{2} NH_3$. The thermogram of this compound is shown in curve 1 of Fig. 12. The first endothermic peak at 130° is due to the loss of water only, and the endo-

Table 8

Composition (mole percent)			Exothermic peak temp.[a] °C	Endothermic peak temp.[b] °C	Surface area (m^2/g)	Process yield of butadiene, percent
Al_2O_3	Cr_2O_3	Fe_2O_3				
80	5	15	—	315—325	330.9	34.92
80	10	10	—	315—325	330.5	19.86
80	15	5	—	315—325	317.0	25.89
60	10	30	—	315—325	309.8	26.33
60	30	10	—	315—325 220—250[c]	302.7	26.92
60	20	20	—	315—325	282.8	10.77
40	30	30	—	220—250[c] 315—325	310.9	27.24
20	40	40	650	—	301.9	13.90
40	40	20	—	220—250[c] 315—325	276.3	21.90
30	30	40	—	220—250[c] 315—325	260.0	18.71
20	20	60	—	—	258.9	18.58
10	10	80	625	—	230.1	14.71
40	20	40	—	320	302.8	24.27
30	40	30	650	—	312.8	24.74
20	60	20	570	—	221.3	7.73
10	80	10	450—500	—	249.5	13.30

a Due to crystallization
b Due to formation of γ-Al_2O_3
c Due to formation of δ-Cr_2O_3

thermic peak at 360° owes its origin to a complex dehydration and decomposition reaction. The overall endothermic reactions can be written as follows:

$$\begin{tikzcd}
SnV_2O_7 \cdot 2\tfrac{1}{2}\, H_2O \cdot \tfrac{1}{2}\, NH_3 \arrow[r, "-1\tfrac{1}{2}\, H_2O", "\text{at } 130^\circ"'] & SnV_2O_7 \cdot H_2O \cdot \tfrac{1}{2}\, NH_3 \arrow[d, "-\tfrac{1}{2}\, NH_3"', "-H_2O \ \text{at } 360^\circ"] \\
SnO_2 + V_2O_5 & SnV_2O_7 \arrow[l, "\text{at } 360^\circ"']
\end{tikzcd}$$

This sequence of reactions has been supported by thermogravimetric studies, X-ray analysis and infrared spectroscopy. The exothermic peak (which is not fully shown in the thermogram) at 420° is considerably suppressed in nitrogen atmosphere and may be due to an oxidation reaction. As in ammonium metavanadate [27], in this case also, ammonia liberated by the decomposition of tin vanadate undergoes oxidative degradation on the surface of V_2O_5 and the subsequent oxidation of the reduced surface in air gives rise to the exothermic peak. The promoter action of SnO_2 over V_2O_5, both formed by the decomposition of tin vanadate, explains the high catalytic activity of tin vanadate in certain oxidation reactions as reported by several workers.

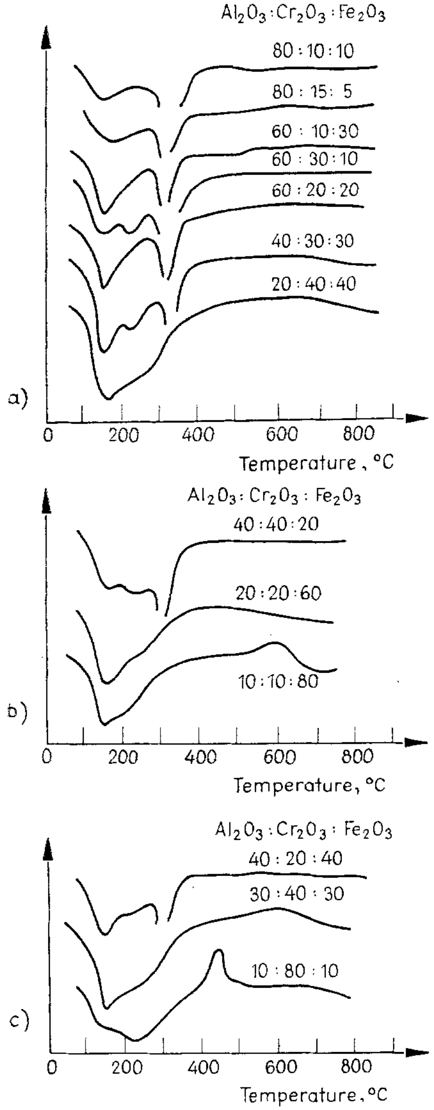

Fig. 11. DTA curves of Al_2O_3—Fe_2O_3—Cr_2O_3 ternary gels

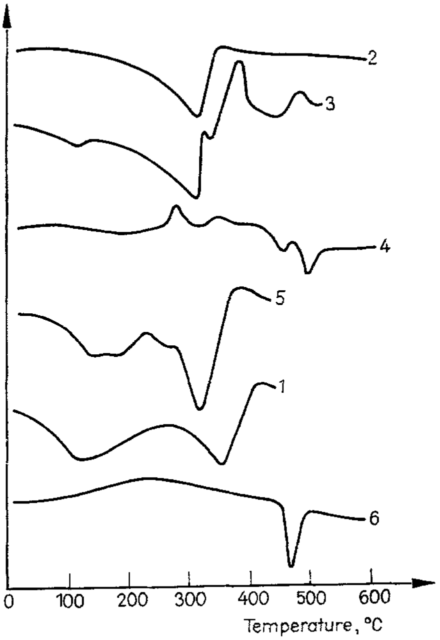

Fig. 12. DTA curves of the vanadates of tin, copper, lead, cobalt and silver

(ii) Copper orthovanadate trihydrate: The DTA thermogram of the compound $Cu_3(VO_4)_2 \cdot 3\,H_2O$ is represented by curve 2 in Fig. 12. The endothermic peak at 320° is due to the dehydration reaction:

$$Cu_3(VO_4)_2 \cdot 3\,H_2O \rightarrow Cu_3(VO_4)_2 + 3\,H_2O$$

No decomposition into component oxides has been detected. X-ray analysis of the fused compound indicated a considerable change in the diffraction pattern of the original compound. This may be due to the formation of a non-stoichiometric compound, $3\,CuO \cdot V_2O_4$, in the fused state [28].

(iii) Copper vanadate: When hot saturated solution of NH_4VO_3 was added to $Cu(NO_3)_2$ solution instead of cold saturated solution of NH_4VO_3 as in the preparation of $Cu_3(VO_4)_2 \cdot 3\,H_2O$, a complex copper vanadate was obtained having the composition: Cu 14.4%, V 32.25%, NH_3 2.17%, H_2O 8.58%.

The thermogram of this compound is shown by curve 3 of Fig. 12 and this resembles that of NH_4VO_3. The endothermic peak at 120° is due to the loss of adsorbed water, while the endothermic peak at 315° is due to liberation of water and to formation of an intermediate with the decomposition of NH_4VO_3 [27]. The exothermic peak at 385° is due to both the oxidative degradation of NH_3 over V_2O_5-surface and the reoxidation of the reduced surface. The small exothermic hump at 480° may be due to a phase change. The presence of NH_4VO_3 and its subsequent decomposition at elevated temperatures ultimately giving a reduced V_2O_5-surface can explain the catalytic activity of copper vanadate shown in a number of reactions.

(iv) Lead vanadate: The compound obtained by adding $NaVO_3$ solution (12.5 g/litre, pH 3–3.5, 40–50°) to 1 *M* $Pb(NO_3)_2$ solution (80°, pH 3) was found to have the composition $Pb_4V_6O_{19} \cdot H_2O$ (Pb 56.35%, V 19.09%, H_2O 1.2%). The thermogram of this compound is shown in curve 4 of Fig. 12. There is a flat endothermic shift in the temperature range 110–265° due to the elimination of water. The thermogram contains two exothermic peaks of small magnitudes at 275° and 350° followed by two endothermic peaks at 460° and 500°. The endothermic peaks are attributed to sintering and melting, respectively, while the exothermic peaks are due to phase changes. X-ray analysis indicates that in the exothermic reaction regions some disorder to order transition takes place, and during melting reversion to the initial disordered form occurs.

(v) Cobalt vanadate: The composition of the compound was found to be $2\,Co(VO_3)_2 \cdot 5\,H_2O$. The thermogram of $2\,Co(VO_3)_2 \cdot 5\,H_2O$ is represented by curve 5 of Fig. 12. X-ray analysis has not indicated the decomposition of the compound into its component oxides at any stage. All the endothermic peaks are due to the stepwise dehydration of the vanadate. Thermogravimetric and derivative thermogravimetric studies suggest the overall dehydration reaction to occur in the following steps:

1) Up to 200°, $2\,\mathrm{Co(VO_3)_2 \cdot 5\,H_2O} \xrightarrow{-1.5\,\mathrm{H_2O}} 2\,\mathrm{Co(VO_3)_2 \cdot 3.5\,H_2O}$.

2) At about 270°, $2\,\mathrm{Co(VO_3)_2 \cdot 3.5\,H_2O} \xrightarrow{-\mathrm{H_2O}} 2\,\mathrm{Co(VO_3)_2 \cdot 2.5\,H_2O}$.

3) At about 315°, $2\,\mathrm{Co(VO_3)_2 \cdot 2.5\,H_2O} \xrightarrow{\quad} \mathrm{Co(VO_3)_2}$.

From X-ray analysis it was found that the crystal structure of the compound changes in the course of dehydration at about 290° and the completely dehydrated sample is less crystalline than the original compound.

(vi) Silver metavanadate: Curve 6 of Fig. 12 represents the DTA thermogram of $\mathrm{AgVO_3}$. Only an endothermic peak at 470° due to fusion is observed in the thermogram.

IV. Conclusion

The thermal behaviour of various oxide systems has been elucidated clearly by the application of DTA technique. It has been found that in case of single oxide systems maximum catalytic activity and maximum surface area correspond to the temperature at which the gel is completely dehydrated and its crystallization starts. In case of mixed oxide systems, a mutual protective action against crystallization is observed, and the composition which develops maximum mutual protective action against crystallization exhibits highest catalytic activity and largest surface area. Vanadates which are useful as catalysts generally contain small percentage of ammonia or ammonium metavanadate as impurities, and the decomposition of ammonium metavanadate and the subsequent degradative oxidation of ammonia, thence liberated, on $\mathrm{V_2O_5}$-surface are important factors in determining their catalytic activity.

It may be concluded that the DTA technique is a simple one and can be used for routine testing of the catalysts employed in industries and laboratories. Though the thermal changes cannot offer a definite clue to the nature of the structural changes in the catalyst systems, the technique can give valuable information and guidance to chemists and physicists. So it can be considered as a valuable adjunct to X-ray diffraction units.

References

1. S. K. Bhattacharyya and V. S. Ramchandran, J. Sci. Industr. Res., 12 (1952) 549, 550.
2. S. K. Bhattacharyya and V. S. Ramchandran, J. Sci. Industr. Res., B12 (1953) 279.
3. S. K. Bhattacharyya and V. S. Ramchandran, J. Sci. Engng. Res. (I. I. T., Kharagpur), 1 (1957) 73.
4. S. K. Bhattacharyya and V. S. Ramchandran, Bull. Nat. Inst. Sci. India, 12 (1959) 23. (Proc. of the Symposium on Contact Catalysis, 1956, Calcutta.)

5. S. K. Bhattacharyya, V. S. Ramchandran and J. C. Ghosh, Adv. in Catalysis, Academic Press Inc., New York, Vol. IX, 1957, p. 114. (Proc. Int. Congr. on Catalysis, 1956, Philadelphia.)
6. S. K. Bhattacharyya and S. Kameswari, Bull. Nat. Inst. Sci. India, 12 (1959) 43.
7. S. K. Bhattacharyya and S. Kameswari, J. Chim. phys., 56 (1959) 823.
8. S. K. Bhattacharyya, S. Kameswari and G. Srinivasan, Z. phys. Chem., 214 (1960) 191.
9. S. K. Bhattacharyya and N. D. Ganguly, Proc. Nat. Inst. Sci. India, 27A (1961) 588.
10. S. K. Bhattacharyya, G. Srinivasan and N. D. Ganguly, J. Indian Chem. Soc., 41 (1964) 233.
11. S. K. Bhattacharyya, Proc. First Int. Congr. Thermal Analysis, Aberdeen, 1965, p. 239.
12. S. K. Bhattacharyya, G. S. De and N. C. Datta, Proc. Second Int. Congr. Thermal Analysis, Worcester, 1968.
13. S. K. Bhattacharyya and J. Ghosh, Proc. Second Int. Congr. Thermal Analysis, Worcester, 1968.
14. Griffith et al., Nature, 172 (1953) 77.
15. Griffith et al., Proc. Roy. Soc., A 224 (1954) 412, 419, 426.
16. M. Domine-Burges, Compt. Rend., 228 (1949) 1435.
17. Berezovskaya and Semikhatova, J. Phys. Chem. (U.S.S.R.), 7 (1936) 939.
18. J. Brenet and A. M. Briot, Compt. Rend., 232 (1951) 1300, 2021.
19. H. Pichler and K. H. Ziesecke, Bull. U.S. Bur. Min., 488 (1950) 34.
20. W. O. Milligan and L. Merten, J. Phys. Coll. Chem., 51 (1947) 521.
21. W. O. Milligan and J. Holmes, J. Am. Chem. Soc., 63 (1941) 149.
22. H. B. Weiser, W. O. Milligan and G. A. Mills, J. Phys. Coll. Chem., 52 (1948) 942.
23. W. O. Milligan and L. Merten, J. Phys. Chem., 50 (1946) 465.
24. R. P. Eischens and P. W. Selwood, J. Am. Chem. Soc., 70 (1948) 227.
25. A. G. Oblad, T. H. Milliken and G. A. Mills, Adv. in Catalysis, Academic Press Inc., New York, Vol. III, 1951, p. 199.
26. V. N. Ipatieff and G. S. Monroe, J. Am. Chem. Soc., 61 (1945) 2168.
27. M. Taniguchi and T. R. Ingraham, Can. J. Chem., 42 (1964) 2467.
28. N. Strupler, Compt. Rend., 255 (1962) 527.

Résumé — On a examiné les principales caractéristiques du comportement thermique des catalysateurs suivants, avec systèmes d'oxydes hétérogènes:

(A) Systèmes d'oxydes simples: 1. Cr_2O_3, 2. Fe_2O_3, 3. Al_2O_3, 4. MnO_2, 5. ZrO_2, 6. NiO, 7. ZnO, 8. TiO_2, 9. SiO_2, 10. ThO_2;

(B) Systèmes d'oxydes binaires: 1. Cr_2O_3—Al_2O_3, 2. Cr_2O_3—Fe_2O_3, 3. Cr_2O_3—ZnO, 4. Al_2O_3—SiO_2, 5. Al_2O_3—Fe_2O_3, 6. MnO—Cr_2O_3, 7. Cu—Al_2O_3 8. ZrO_2—Cr_2O_3, 9. NiO—Cr_2O_3, 10. ZrO_2—NiO, 11. ThO_3—Al_2O_3;

(C) Systèmes d'oxides ternaires: 1. NiO—Cr_2O_3—ZrO_2; 2. Fe_2O_3—Cr_2O_3—Al_2O_3;

(D) Vanadates: 1. d'étain, 2. de cuivre, 3. de plomb, 4. de cobalt, 5. d'argent.

Les caractéristiques thermiques des solides, observées par A. T. D., montrent une bonne concordance avec leurs surfaces spécifiques et leur activité catalytique.

Zusammenfassung — Es wurden die wichtigsten Kennzeichen des thermischen Verhaltens folgender heterogener Katalysator-Systeme untersucht.

(A) Einfache Oxydsysteme: 1. Cr_2O_3, 2. Fe_2O_3, 3. Al_2O_3, 4. MnO_2, 5. ZrO_2, 6. NiO, 7. ZnO, 8. TiO_2, 9. SiO_2, 10. ThO_2.

(B) Binäre Oxydsysteme: 1. Cr_2O_3—Al_2O_3, 2. Cr_2O_3—Fe_2O_3, 3. Cr_2O_3—ZnO, 4. Al_2O_3—SiO_2, 5. Al_2O_3—Fe_2O_3, 6. MnO—Cr_2O_3, 7. Cu—Al_2O_3, 8. ZrO_2—Cr_2O_3, 9. NiO—Cr_2O_3, 10. ZrO_2—NiO, 11. ThO_2—Al_2O_3.

(C) Ternäre Oxydsysteme: 1. NiO—Cr_2O_3—ZrO_2, 2. Fe_2O_3—Cr_2O_3—Al_2O_3.

(D) Vanadate: 1. Zinn-, 2. Kupfer-, 3. Blei-, 4. Kobalt-, 5. Silbervanadate.

Gute Übereinstimmung konnte zwischen den durch DTA Messungen gefundenen thermischen Kennzeichen der festen Substanzen und ihren spezifischen Oberflächen, sowie der katalytischen Aktivität festgestellt werden.

Резюме. — Исследованы характерные свойства термического поведения следующих систем:

(А) Одинарные системы окисей: (I) Cr_2O_3, (II) Fe_2O_3 (III) Al_2O_3, (IV) MnO_2, (V) ZrO_2, (VI) NiO, (VII) ZnO, (VIII) TiO_2, (IX) SiO_2, (X) ThO_2.

(Б) Бинарные системы окисей: (I) Cr_2O_3— Al_2O_3, (II) Cr_2O_3— Fe_2O_3, (III) Cr_2O_3— ZnO, (IV) Al_2O_3— SiO_2, (V) Al_2O_3— Fe_2O_3, (VI) MnO— Cr_2O_3, (VII) Cu— Al_2O_3, (VIII) ZrO_2— Cr_2O_3, (IX) NiO— Cr_2O_3, (X) ZrO_2— NiO, (XI) ThO_2— Al_2O_3.

(В) Тройные системы окисей: (I) NiO— Cr_2O_3— ZrO_2, (II) Fe_2O_3— Cr_2O_3— Al_2O_3.

(Г) Ванадаты: (I) ванадат олова, (II) ванадат меди, (III) ванадат свинца, (IV) ванадат кобальта, и (V) ванадат серебра.

В большинстве систем методом дифференциального термического анализа (ДТА) найдена отличная корреляция, между термическими характеристиками исследуемых веществ, их поверхностью и каталитической активностью.